An improved method for location of microseismic events with low signal-to-noise ratios

Yuyang Tan[*]
Peking University
Beijing, China
t150293@pku.edu.cn

Chuan He
Peking University
Beijing, China
chuanhe_pku@163.com

Xiaochen Hou
Peking University
Beijing, China
1201210320@pku.edu.cn

SUMMARY

An improved method is proposed in this paper for microseismic source location. The primary goal of this method is to improve the location accuracy for microseismic events with low signal-to-noise ratios (SNR). In contrast to the prevalent location approach, two innovations are implemented in the proposed method. First, instead of using the hodogram, the source azimuth is estimated from a probability distribution function, and second, a new objective function is employed in grid search algorithm to find the source position. The proposed method has been tested using synthetic data examples. The results show that, for these cases, the absolute errors of the estimated source azimuth and position are less than 1° and 3m, respectively, which proves that an improvement in location accuracy can readily be achieved using the proposed method.

Key words: microseismic source location, signal-to-noise ratio, polarization attribute, probability distribution function, objective function, grid search algorithm.

INTRODUCTION

Unconventional oil and gas reservoirs generally exhibit low permeability, thus their production often requires multi-stage hydraulic fracturing to create connected pathways through which oil and gas can flow. Hydraulic fracture stimulation is usually accompanied by the occurrence of numerous small earthquakes, also known as microseismicities. These small earthquakes are important as their locations can be used to understand the fracture geometry and growth, including the orientation and dimensions, and further used to optimize the late-stage treatment (Maxwell, 2010).

Microseismic sources typically are located using the P- and S-wave arrival times of microseismic events and the velocity model between treatment and monitoring wells. Prevalent location approach generally consists of two steps: the first step is to estimate the source azimuth based on P-wave polarization, and the second step is to search for the source position by minimizing the discrepancy between the observed and predicted arrival times (De Meersman *et al.*, 2009). Our method can be considered as an improvement of the prevalent approach, since two innovations are implemented in this method to improve the location accuracy for the low SNR microseismic events. The performance of the proposed method will be illustrated using synthetic data examples.

METHOD

Conventional location approach first requires calculating the back-azimuth to the source. The azimuth is usually estimated from P-wave hodogram, which is a 2D plot of the particle motion of two horizontal components of the P-wave. It is easy to determine this angle when the hodogram is nearly linear, but in actual situations, the linearity of the hodogram is usually deteriorated by the ambient noises, which could result in an unreliable estimate of the source azimuth. To mitigate the influence of the ambient noises, a probability distribution function is defined and used to determinate the source azimuth in our method. Computation of this function first requires a polarization analysis approach applied to estimate the P-wave polarization attributes, namely the degree of polarization P and the angle of strike α for 2-component dataset (Flinn, 1965). The expressions of P and α are

$$P = 1 - \frac{\lambda_2}{\lambda_1}, \tag{1}$$

$$\alpha = \tan^{-1}\left(\frac{u_y}{u_x}\right) \tag{2}$$

where λ_1 and λ_2 ($\lambda_1 > \lambda_2$) denote the eigenvalues of a covariance matrix constructed using two horizontal components of the P-wave waveform data, and $\mathbf{u}_1 = [u_x, u_y]$ is the eigenvector associated with λ_1. The value of P lies in the interval of 0~1, with $P=0$ indicating circular hodogram while $P=1$ indicating linear hodogram. With P and α, the probability distribution function is defined as

$$F_{pdf} = \frac{\lambda P}{\sqrt{2}} e^{-\frac{\lambda^2 P^2 (\alpha-\theta)^2}{2}}, \tag{3}$$

where θ is a series of angles beginning from $-\pi/2$ to $\pi/2$ with a sampling interval of 0.0001, and λ is a control parameter which can modulate the shape (height and width) of this function. In practice, this probability distribution function is first computed for each trace in the record, and then summed up to formulate one global function. The maximum of this global function is interpreted as the optimal estimate of the source azimuth.

In the next step, the microseismic source is located in a 2D vertical plane determined by the source azimuth using grid search algorithm. The definition of the objective function in grid search algorithm is a key element, as it determines the accuracy of the location result. Conventional location approach defines the objective function as the residual of the observed and predicted P- or S-wave arrival times. However, this objective function is very sensitive to the pick errors within the observed arrival times and could result in a mis-location if the

pick errors are large. So in our method, a new objective function is employed to minimize the impact of the pick errors. Assuming that T_p^i, T_s^i represent the observed P- and S-wave arrival times and t_p^i, t_s^i represent the calculated P- and S-wave travel times, the objective function is then defined as

$$F_{obj} = \gamma \sum_{i=1}^{M} \left[(T_p^i - t_p^i - T_o)^2 + (T_s^i - t_s^i - T_o)^2 \right] / 2$$

$$+ (1-\gamma) \sum_{i=1}^{M} \left[(T_p^i - T_s^i) - (t_p^i - t_s^i) \right]^2, \quad (4)$$

in which

$$T_o = \frac{1}{M} \sum_{i=1}^{M} \left[(T_p^i - t_p^i) + (T_s^i - t_s^i) \right] / 2, \quad (5)$$

where M is the number of downhole receivers and γ is a weighting factor between 0 and 1. Equation (4) will be proved later that it is less sensitive to the pick errors, and this property is of great significance because the pick errors are usually large for the low SNR microseismic events. The microseismic source position is then located by searching for the global minimum of the objective function.

EXAMPLES

The first synthetic data example illustrates the accuracy of the probability distribution function in determination of the source azimuth. Figure 1 shows two horizontal components of the P-wave of a synthetic microseismic event. The ambient noises in this dataset are simulated by normally distributed random numbers and the average signal-to-noise ratio of the traces is 2.56dB. The real source azimuth of this event is set to be 45°. Table 1 lists the calculated polarization attributes of each trace within the synthetic dataset and Figure 2 displays the probability distribution functions computed using these attributes. For comparison purpose, the hodogram of each trace is also shown in this figure. As one can see from Figure 2 that, with the decrease of the P value, the shape of the probability distribution function becomes low and flat. This variation is reasonable since high value of P suggests that the hodogram is nearly linear, so its principal axis is obvious and its direction has small uncertainty. However, if P has a low value, that means the hodogram is elliptical and the direction of its principal axis will show a relatively large uncertainty. Figure 3 shows the normalized global function obtained by summing up all probability distribution functions in Figure 2. The azimuth corresponding to the maximum (denoted by the red asterisk) of the global function is 44.3°, which shows a discrepancy less than 1° with respect to the real value.

In the second example, the effectiveness of the new objective function in source location is illustrated. The physical model used in this example is a four-layer flat-bedded model whose parameters are listed in Table 2. The coordinates of the true position of a microseismic source are set to be [50m, 2250m]. Figure 4 displays the assumed positions of the microseismic source and downhole receivers. The raypaths of the P- and S-wave (also shown in Figure 4) are calculated using a ray-tracing

algorithm and their arrival times (as shown in Figure 5) are generated by adding 10 seconds to the calculated travel times. In addition, a set of random numbers are also added to the synthetic arrival times to simulate the pick errors. For this example, the search ranges of the grid search algorithm are set to be 0~100m for distance and 2200~2300m for depth, and the grid interval is 1m. Figure 6 displays the location result obtained by employing the new objective function in grid search algorithm. The estimated source position (denoted by the green cross) is located at [49m, 2247m], and one can see from Figure 6 that it is very close to the true position (denoted by the red circle). The deviation between these two positions is about 3m.

Table 2 Parameters of the physical model shown in Fig.4

Layer	Depth (m)	P-wave velocity (m/s)	S-wave velocity (m/s)
1	2000~2100	1600	1000
2	2100~2150	2000	1300
3	2150~2300	2400	1600
4	2300~2400	2800	1900

CONCLUSIONS

This paper presents an improved method for location of microseismic events with low signal-to-noise ratios. Innovations in this method include the use of a probability distribution function for estimation of the source azimuth and a new objective function for determination of the source position. Application of the proposed method on synthetic data examples demonstrates that it is less susceptible to the ambient noises and pick errors, thereby an improvement in location accuracy can readily be achieved using this method.

ACKNOWLEDGMENTS

REFERENCES

De Meersman, K., Kendall, J.M., and van der Baan, M., 2009, The 1998 Valhall microseismic data set: An integrated study of relocated sources, seismic multiplets, and S-wave splitting: Geophysics, 74, B183-B195.

Flinn, E.A., 1965, Signal analysis using rectilinearity and direction of particle motion: Proceedings of the IEEE, 53, 1874-1876.

Maxwell, S.C., 2010, Microseismic: Growth born from success: The Leading Edge, 29, 338-343.

Table 1   Polarization attributes of the synthetic dataset shown in Fig.1

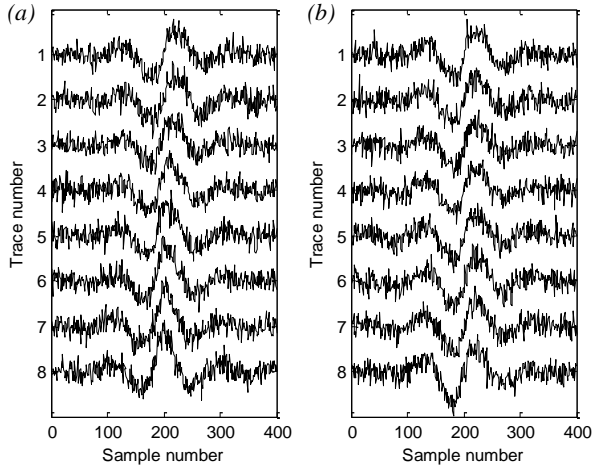| Trace No.	1	2	3	4	5	6	7	8
P	0.452	0.362	0.270	0.248	0.141	0.058	0.031	0.019
α	44.9°	44.0°	46.4°	40.7°	40.5°	39.7°	37.3°	36.9°

Figure 1   Two horizontal components of the P-wave of a synthetic microseismic event. (a) X-component, (b) Y-component.
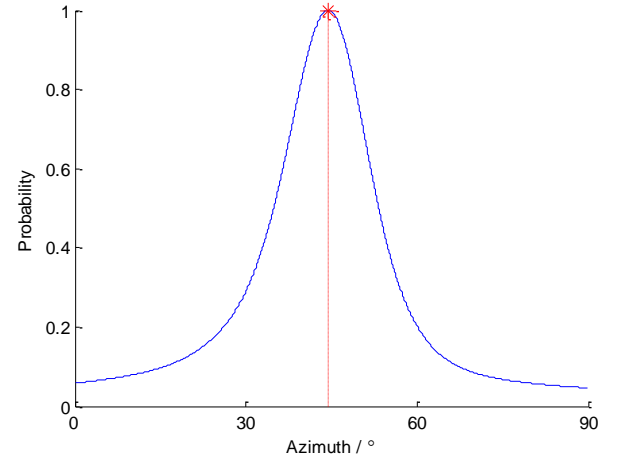
Figure 3   Normalized global function. In this figure, the maximum point of the global function is denoted by the red asterisk.
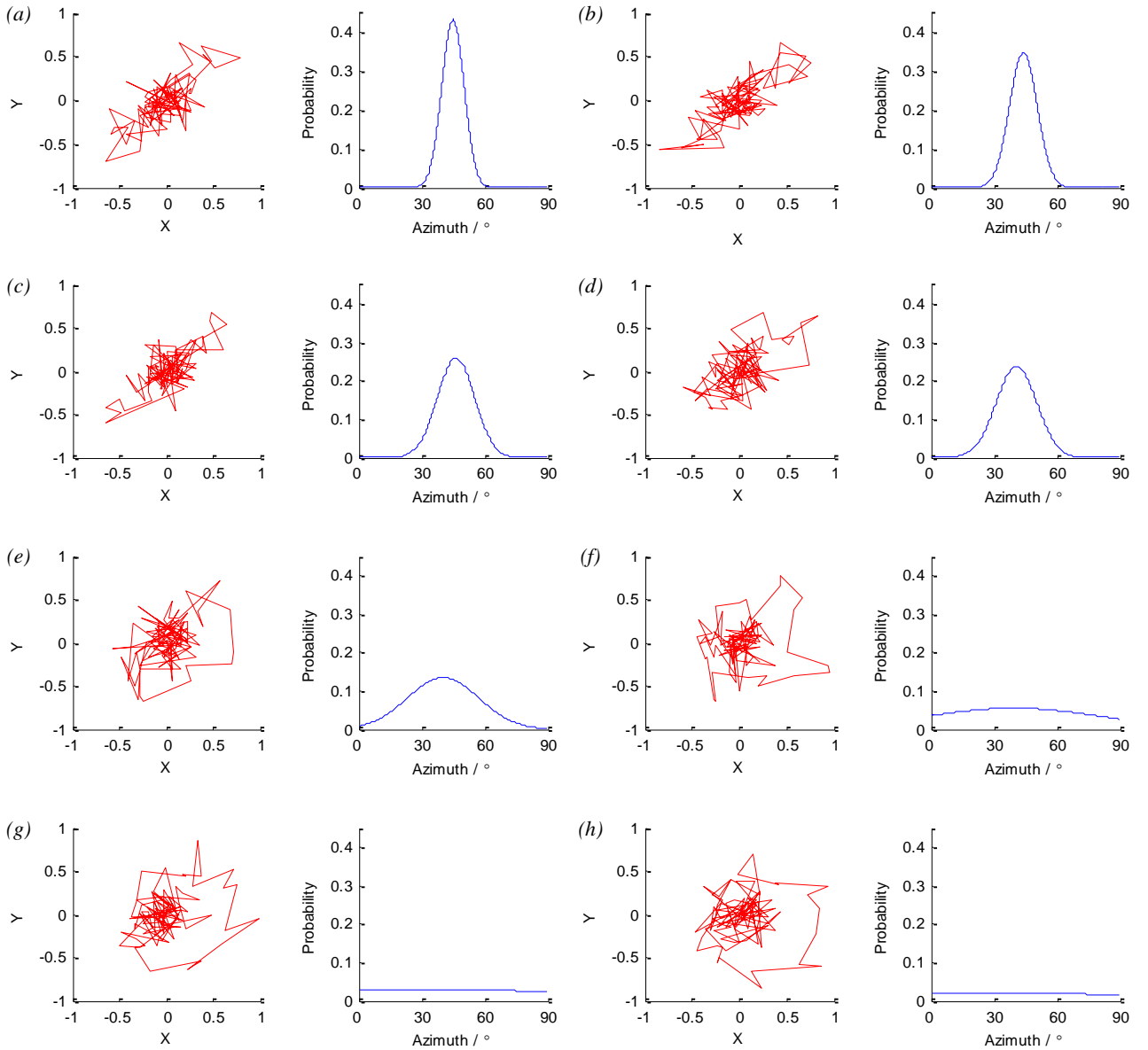

Figure 2   Hodograms and probability distribution functions of all traces shwon in Fig.1. (a)~(h) denote the results for Trace 1~8, respectively.
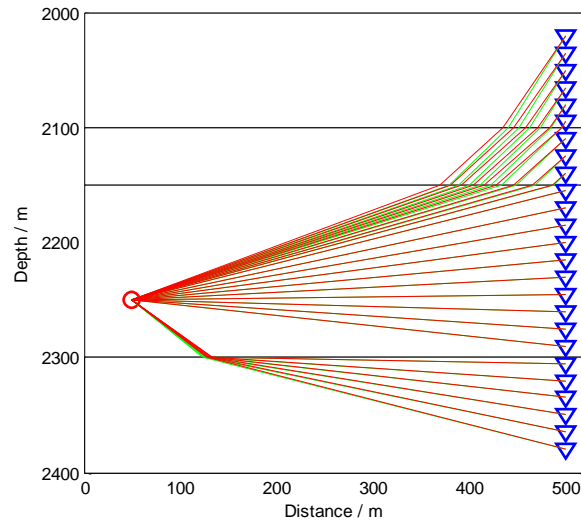
Figure 4   Positions of the microseismic source (red circle) and downhole receivers (blue inverse triangles), and raypaths of the P-wave (red lines) and S-wave (green lines).
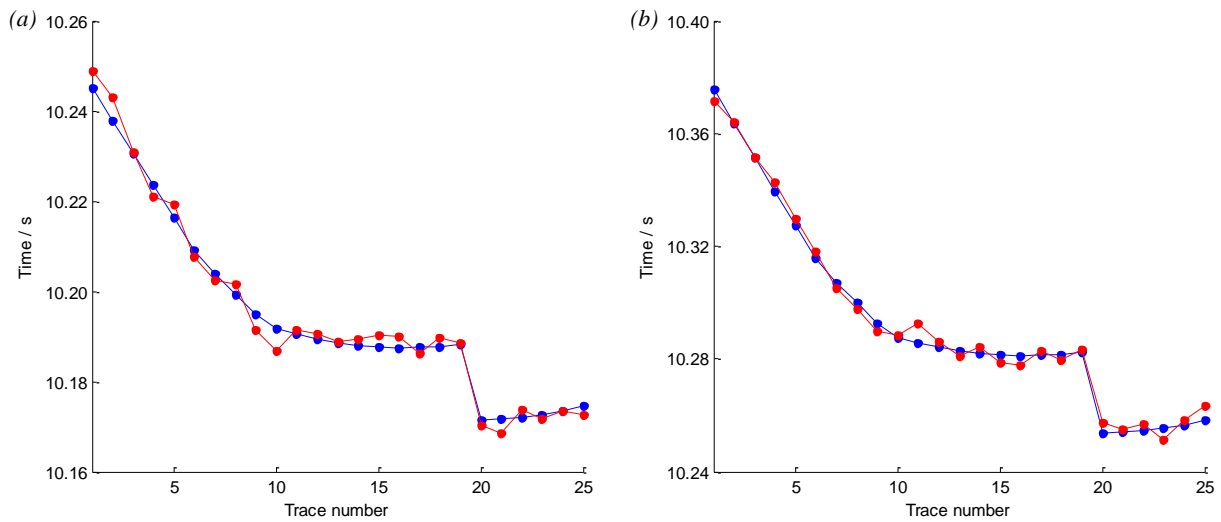

Figure 5   Synthetic arrival times of different phases. (a) P-wave, (b) S-wave. In each figure, the blue dot line denotes the arrival times without pick errors and the red dot line denotes the arrival times with pick errors.
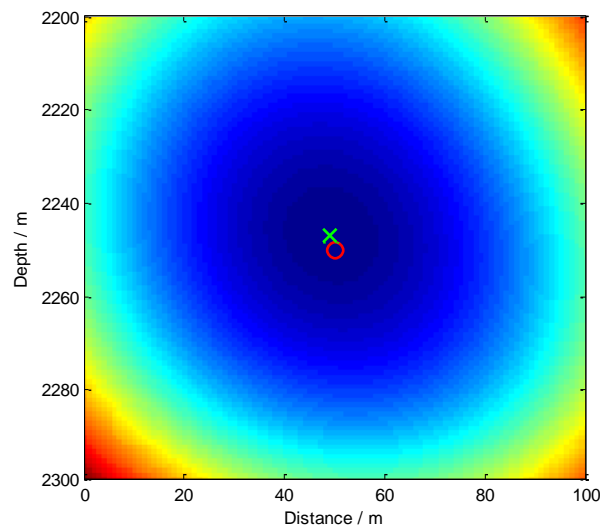

Figure 6   Source location result obtained using the new objective function and grid search algorithm. In this figure, the values of the objective function are denoted by different colors, the true and estimated positions of the microseismic source are denoted by the red circle and green cross, respectively.